5,12-Dialkyl-5,12-dihydroindolo[3,2- a]carbazole-Based Oxime-Esters for LED Photoinitiating Systems and Application on 3D Printing

Fatima Hammoud, Nicolas Giacoletto, Malek Nechab, Bernadette Graff, Akram Hijazi, Frédéric Dumur, Jacques Lalevée

▶ **To cite this version:**

Fatima Hammoud, Nicolas Giacoletto, Malek Nechab, Bernadette Graff, Akram Hijazi, et al.. 5,12-Dialkyl-5,12-dihydroindolo[3,2- a]carbazole-Based Oxime-Esters for LED Photoinitiating Systems and Application on 3D Printing. Macromolecular Materials and Engineering, 2022, pp.2200082. 10.1002/mame.202200082 . hal-03712520

HAL Id: hal-03712520
https://hal.science/hal-03712520

Submitted on 4 Jul 2022

HAL is a multi-disciplinary open access archive for the deposit and dissemination of scientific research documents, whether they are published or not. The documents may come from teaching and research institutions in France or abroad, or from public or private research centers.

L'archive ouverte pluridisciplinaire **HAL**, est destinée au dépôt et à la diffusion de documents scientifiques de niveau recherche, publiés ou non, émanant des établissements d'enseignement et de recherche français ou étrangers, des laboratoires publics ou privés.

5,12-Dialkyl-5,12-dihydroindolo[3,2-*a*]carbazole-based oxime-esters for LED photoinitiating systems and application on 3D printing

Fatima Hammoud[1,2,3], Nicolas Giacoletto[4], Malek Nechab[4], Bernadette Graff[1,2], Akram Hijazi[3], Frédéric Dumur[4*] and Jacques Lalevée[1,2*]

[1] Université de Haute-Alsace, CNRS, IS2M UMR7361, F-68100 Mulhouse, France.

[2] Université de Strasbourg, France.

[3] EDST, Université Libanaise, Campus Hariri, Hadath, Beyrouth, Liban.

[4] Aix Marseille Univ, CNRS, ICR, UMR 7273, F-13397 Marseille, France.

Corresponding authors: Frederic.dumur@univ-amu.fr; jacques.lalevee@uha.fr

Abstract:

In order to expand the application of oxime-esters (OXEs) and to introduce a one-component photoinitiating system of high performance in visible light photopolymerization, we designed and synthetized a series of 5,12-dihexyl-5,12-dihydroindolo[3,2-*a*]carbazole-based oxime-esters with visible absorption abilities. Notably, when irradiated with light-emitting diodes at 405 nm, the proposed structures could undergo a direct cleavage of the N-O bond followed by decarboxylation, generating free radicals capable to efficiently initiate free radical photopolymerizations (FRP). Furthermore, the new OXEs showed good thermal initiation abilities and could be used as dual photo and thermal initiators. An interesting structure/reactivity/efficiency relationship could be obtained by comparing the reactivity of the different radicals generated upon photoexcitation at identical chromophore but also by comparing the photoinitiating ability of our series of dyes with that of another series of dyes designed to exhibit a lower solubility in resins. Indeed, solubility of dyes can constitute a major issue adversely affecting the photoinitiating ability. Chemical mechanisms were studied through different techniques including real-time Fourier Transform Infrared Spectroscopy (RT-FTIR), UV-visible absorption spectroscopy, fluorescence (time-resolved or steady state) as well as molecular modelling calculations. Eventually, the usage of the investigated OXEs in new photosensitive 3D printing resins is also presented.

Keywords: Oxime-esters, visible light, photoinitiators, dual initiators, 5,12-dialkyl-5,12-dihydroindolo[3,2-*a*]carbazole

1. Introduction

The oxime-ester functionality has been identified in a very large number of bioactive compounds and they have been reported as exhibiting antioxidant, antibacterial, anti-inflammatory, anti-diabetes and cytotoxic activities. These structures are also important starting materials for the preparation of photosensitive compositions. [1-3] Several studies have clearly shown their abilities to act as photosensitizers or photoinitiators in light-curing processes. [4-8] Their high efficiency is assigned to the direct photocleavage of the N-O bond, enabling to generate iminyl and acyloxy radicals, which in turn can undergo further decarboxylation reactions. [9,10]

Photochemical polymer production exhibits several advantages that make it more environmentally friendly than the other technologies: It is solvent-free, consumes less energy, cheap and fast. Therefore, this technique is currently widely used for the preparation of composites, coatings, adhesives, 3D printing and so on. [11-16] Indeed, the photoinitiator (PI) is the key component which can produce active species alone or with additives to initiate the polymerization of monomers under light irradiation. [17-18] Generally, a one-component photoinitiating system (Type I photoinitiators) is more advantageous compared to a multicomponent system, as the light-induced direct homolytic cleavage is a more straightforward mechanism to generate the initiating species. Furthermore, the photoinitiating systems also play a pivotal role by controlling the spectral sensitivity of the photopolymerization reactions. [19]

There are two known commercial oxime photoinitiators (Irgacure OXE-01 and OXE-02) that have been used in industrial applications. However, these compounds require high-intensity UV light sources, which can be harmful for the environment and human health. [20-22] Thus, for soft irradiation conditions, the search of new photoinitiators which absorb visible light, remains a great challenge and attracts more and more attention in recent years.

In this context, as visible and safe light sources, light-emitting diodes (LEDs) are a promising alternative to the conventional irradiation setups due to their low costs, compacity, lightweight, long lifetimes. Nowadays, these devices are also easily accessible. [23-25] Recently, several researches have been realized, in order to shift the absorption wavelength of oxime esters towards the visible range, for a better matching of their absorptions with the emission of the

different LED light sources. Different chromophores were examined such as coumarins, [10,20,22,26] phenothiazines, [27] triphenylamines, [9,24,28] and carbazoles. [29-31] From the chemical modification viewpoint, carbazole is an interesting scaffold for the design of visible light Type I and Type II photoinitiators. Indeed, carbazole possesses two reactive positions, namely the 3 and 6-positions, enabling to introduce various functional groups. This strategy can also be applied to 5,12-dialkyl-5,12-dihydroindolo[3,2-a]carbazole. In this case, the most reactive positions of this polyaromatic structure are undoubtedly the 2 and 9-positions. Notably, acetyl groups can easily be introduced by mean of a Friedel-Crafts reaction. After suitable modifications, the acetyl group can be converted as an oxime, opening the way to the synthesis of oxime esters. By the double substitution of 5,12-dialkyl-5,12-dihydroindolo[3,2-a]carbazole, a double source of radicals can be obtained, resulting from the simultaneous presence of two oxime ester group per molecule.

In the present work, a series of 5,12-dihexyl-5,12-dihydroindolo[3,2-*a*]carbazole-based oxime-esters were synthesized and proposed as high-performance photoinitiating systems. Photoreactivity of the investigated compounds were examined upon exposure of the resins to LED@405 nm, also their thermal initiating behaviors were evaluated via differential scanning calorimetry (DSC). Interestingly, a structure performance relationship could be established by examining 1) the difference of photoinitiating ability of the different radicals generated upon irradiation 2) by examining the impact of the solubility of dyes on the photoinitiating ability. Additionally, and in order to highlight their high performance in photopolymerization, their use in photosensitive 3D printing resins upon exposure at 405 nm is presented.

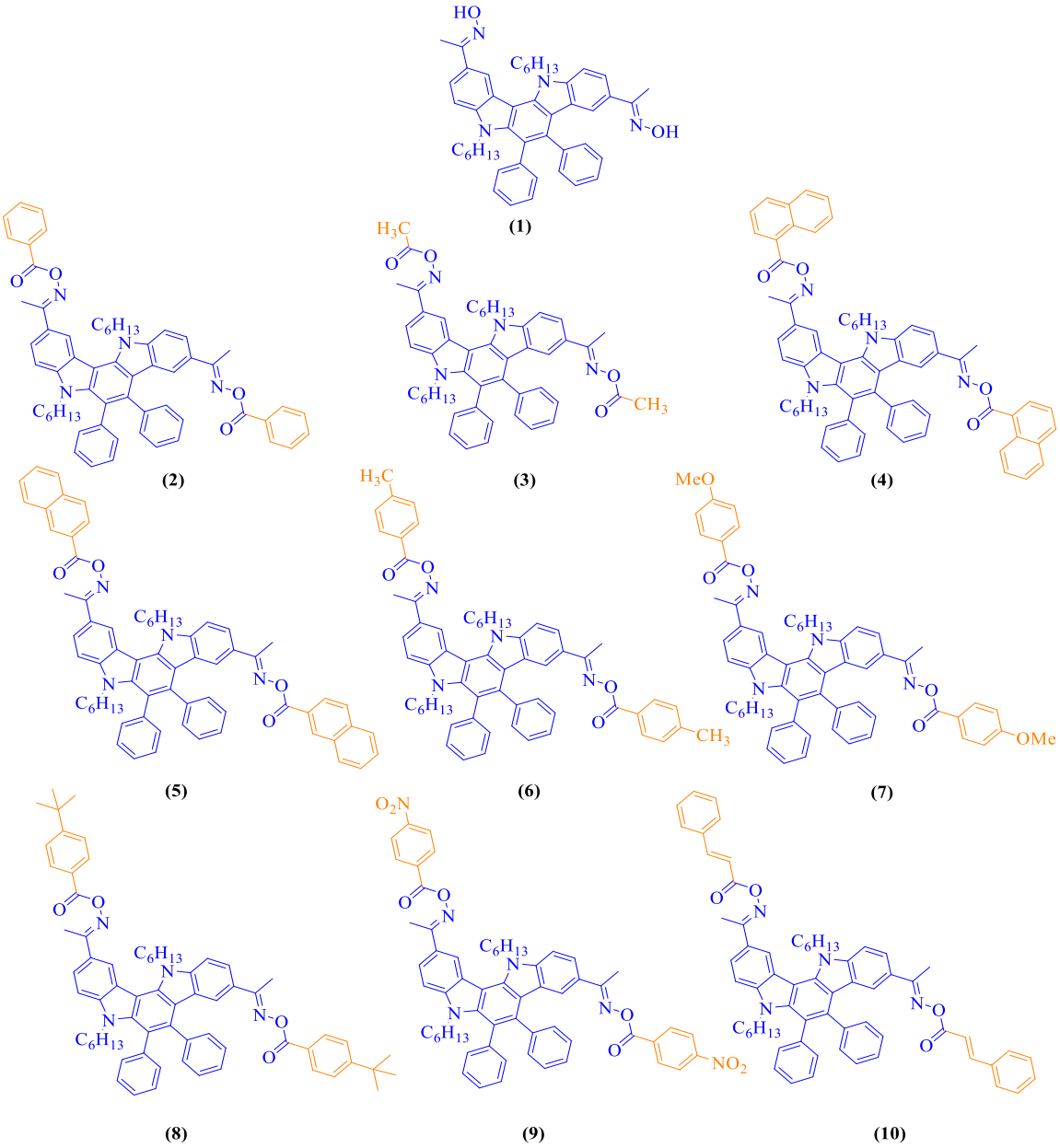

Scheme 1. Chemical structures of the synthetized 5,12-dihexyl-5,12-dihydroindolo[3,2-*a*]carbazole-based oxime-esters **(1)-(10).**

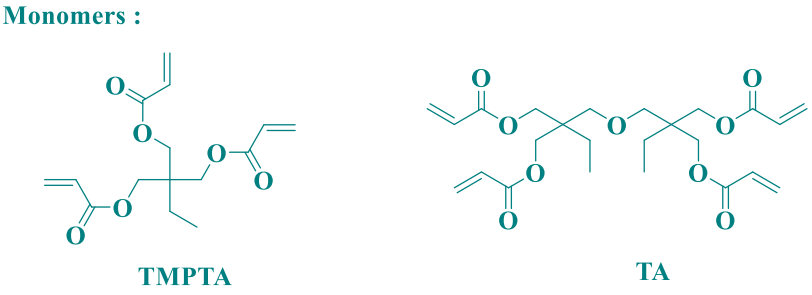

Scheme 2. Chemical structure of monomers used in this work.

2. Experimental part

2.1. Synthesis of the investigated 5,12-dialkyl-5,12-dihydroindolo[3,2-a]carbazole-based oxime-esters

Synthesis of the different oxime esters examined in this work is depicted in Supporting Information.

2.2. Other Chemicals compounds

The monomers were obtained from Allnex. Chemical structures of monomers are shown in Scheme 2.

2.3. Irradiation Source

The following light emitting diodes (LEDs) were used as irradiation sources: (i) λ_{em} = 405 nm (denoted LED@405 nm) with an incident light intensity at the sample surface; I_0 = 110 mW.cm^{-2} and (ii) λ_{em} = 375 nm (denoted LED@375 nm); I_0 = 40 mW.cm^{-2}.

2.4. UV-visible absorption and photolysis experiments

UV-visible absorption properties of the different compounds as well as the steady state photolysis were studied using a JASCO V730 UV-visible spectrophotometer.

2.5. Photopolymerization kinetics (RT-FTIR)

Experimental conditions for each photosensitive formulation are indicated in the caption of the figures. All polymerization experiments were performed at room temperature and the irradiation was started after t = 10 s. The weight of the photoinitiating system was calculated from the monomer content. The conversions of the acrylate functions of the TMPTA were continuously followed by real time FTIR (RT-FTIR) spectroscopy (JASCO FTIR 4100). Photopolymerization experiments were carried out in laminate (the formulation is sandwiched between two polypropylene films (thickness ~ 25 µm) to reduce the O_2 inhibition). Decrease of

the C=C double bond peak was continuously monitored from 1581 to 1662 cm^{-1}. For the thicker samples (1.4 mm of thickness), the formulations were deposited on a polypropylene film inside a 1.4 mm mold under air. Evolution of the C═C bond was continuously followed from 6117 to 6221 cm^{-1}, respectively. The procedures were described by us in references [23-24].

2.6. Computational procedure

Molecular orbital calculations were carried out using the Gaussian 03 suite of programs. Electronic absorption spectra for the different compounds were calculated with time-dependent density functional theory at the MPW1PW91/6-31G* level of theory on the relaxed geometries calculated at the UB3LYP/6-31G* level of theory. Triplet state energy levels were calculated at this level of theory after full optimization of the excited state.

2.7. Fluorescence experiment

Steady state fluorescence. Fluorescence spectra were acquired in a quartz cell at room temperature using a JASCO FP-750 spectrofluorometer.

Time correlated single photon counting (TCSPC). Fluorescence excited state lifetimes were determined using a time correlated single-photon counting system, a HORIBA DeltaFlex with a HORIBA PPD-850 as detector. The excitation source is a HORIBA nanoLED-370 with an excitation wavelength of 367 nm and a pulse duration inferior to 1.4 ns. The fluorescence intensity decay profiles were recorded in acetonitrile in a quartz cell. A silica colloidal solution LUDOX was used to evaluate the impulse response function (IRF) of the apparatus.

2.9. Differential Scanning Calorimetry (DSC) For Thermal Polymerization

About 10 mg of TMPTA containing 1% w oxime-ester initiator (OXE) was inserted into a 100 µL aluminum crucible. Thermal polymerization was performed from room temperature to 300 °C at a heating rate of 10 °C/min. under nitrogen flow (100 mL/min.). A Mettler Toledo DSC 1 differential scanning calorimeter was used.

2.10. Direct Laser Write and 3D printing experiment

For direct laser write experiments, a laser diode @405 nm (spot size around 50 µm) was used for the spatially controlled irradiation. The photosensitive resin was polymerized under air and the generated 3D patterns were analyzed using a numerical optical microscope (DSX-HRSU from Olympus Corporation) as presented in the references [17,25]. For 3D printing, a low light intensity 3D printer (LCD-based 405 nm 3D Printer Anycubic Photon S) was used.

3. Results and discussion

3.1. Synthesis of the different dyes

The different oxime esters ~~**(2)-(10)**~~ investigated in this work could be obtained through a five steps synthesis described in the scheme 3. In order to investigate the impact of the solubility of oxime esters on the monomer conversions, two series of oxime esters were developed in parallel, varying by the length of the alkyl chains introduced at the 5,12 positions of the chromophore. The first step consisted in a cycloaddition reaction between indole and benzil, providing the intermediate **I-1** in 77% yield. **I-1** was then alkylated with iodohexane or with iodomethane in the presence of a base to furnish **I-2** or **I-2'** with excellent yields, respectively 88% and 91%. Next step consisted in a Friedel-Craft reaction involving 5,12-dihexyl-6,7-diphenyl-5,12-dihydroindolo[3,2-*a*]carbazole **I-2** or 5,12-dimethyl-6,7-diphenyl-5,12-dihydroindolo[3,2-*a*]carbazole **I-2'** and acetyl chloride in the presence of aluminum chloride. Intermediates **I-3** and **I-3'** could be obtained in 66% and 76% yield respectively. Then, oximes **(1)** or **(1')** could be synthesized by condensing hydroxylamine hydrochloride on **I-3** or **I-3'** in the presence of sodium acetate as the base and by using a mixture of three solvents (MeOH, THF and H_2O). Oximes **(1)** and **(1')** could be obtained in high yield, around 95% for both. Finally, oximes **(1)** and **(1')** could provide the eighteen oxime-esters (**(2)-(10)** and **(2')-(10')**) by esterification with different acid chlorides and in presence of triethylamine. Detailed procedures for each step are presented in ESI. All oxime-esters could be obtained in pure form by a simple precipitation in diethyl ether, with reaction yields ranging from 65 for **(4')** to 89% for **(10)**.

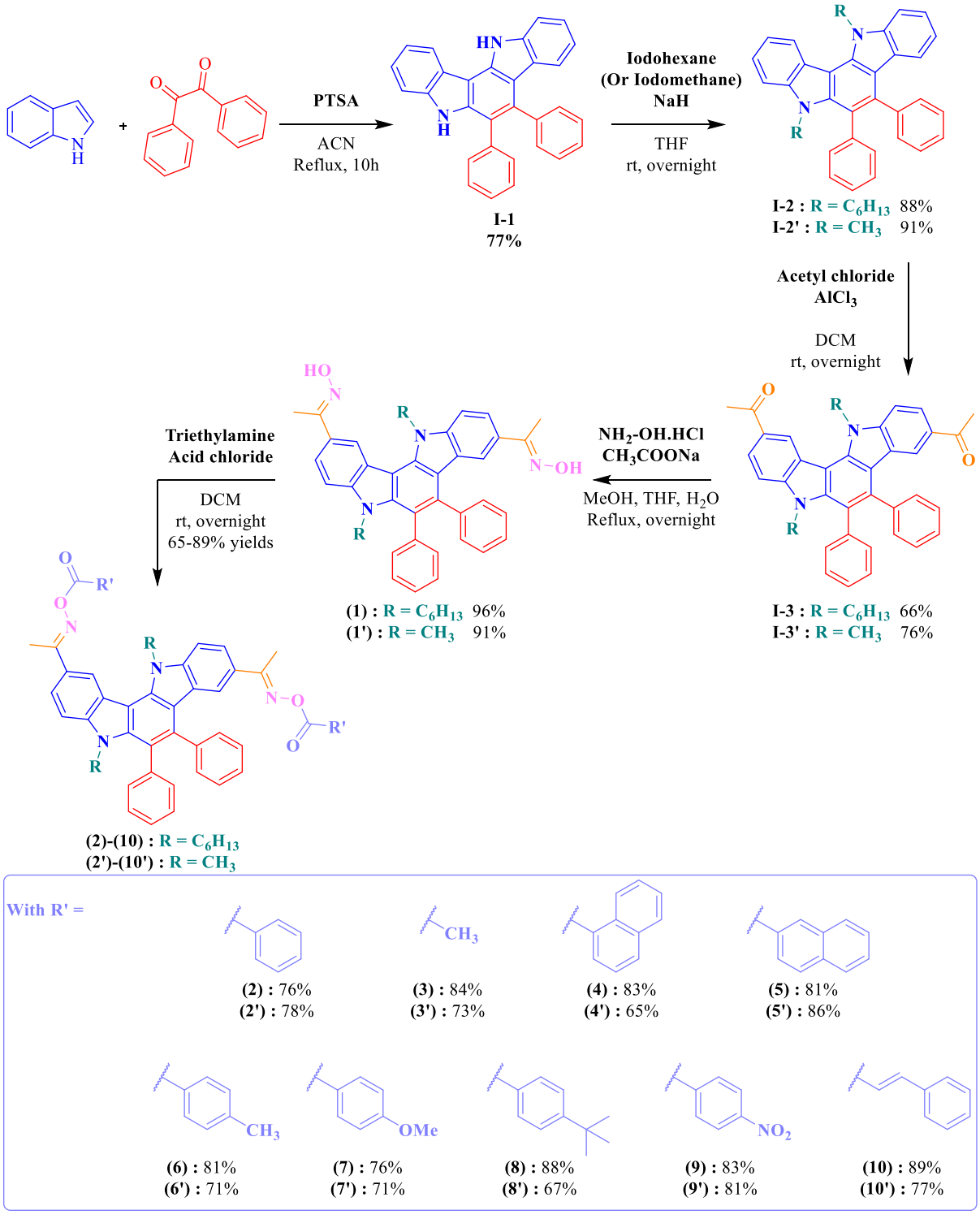

Scheme 3. Synthetic routes to oxime-esters **(1)-(10)** and **(1')-(10')**.

3.2. UV-visible absorption

UV–visible absorption spectra of the new proposed oxime esters **(1)-(10)** (Scheme 1) in toluene are shown in Figure 1. Maximum absorption wavelengths (λ_{max}), extinction coefficients (ε_{max}) at λ_{max} and at the emission wavelength @405 nm are gathered in Table 1.

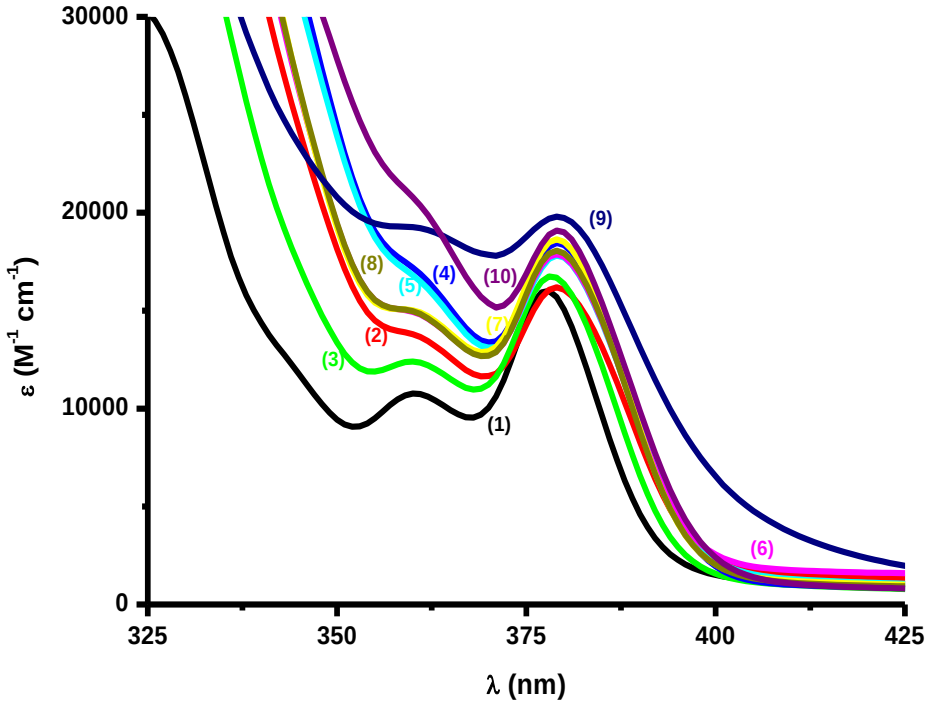

Figure 1. UV-visible absorption spectra of the investigated 5,12-dihexyl-5,12-dihydroindolo[3,2-*a*]carbazole-based oxime-esters **(1)-(10)** in toluene.

Table 1. Light absorption properties of the proposed structures **(1)-(10)**; maximum absorption wavelengths (λ_{max}), extinction coefficients at λ_{max} and extinction coefficients at 405 nm.

PI	λ_{max} (nm)	ε_{max} (M^{-1} cm^{-1})	$\varepsilon_{(405nm)}$ (M^{-1} cm^{-1})
(1)	378	16000	1260
(2)	379	16200	1720
(3)	378	16700	1145
(4)	379	18450	1200
(5)	379	17800	1535
(6)	379	17900	1930
(7)	379	18650	1400
(8)	379	18000	1335
(9)	379	19800	4780
(10)	379	19000	1395

Noticeably, by replacing the hexyl chain of the **(1)-(10)** series by a methyl chain in the **(1')-(10')** series, no modification of the absorption maxima was found between the two series of dyes. According to the results presented in Figure 1 (also Table 1), all the investigated structures exhibited high molar extinction coefficients (values between 16000 and 20000 $M^{-1}.cm^{-1}$)). Therefore, the absorption properties of the different oxime-esters allowed a good overlap with the emission spectra of the visible LED used in this work.

3.3. Free radical photopolymerization in TMPTA

Photoinitiation abilities of the different oxime-esters (0.5% w) based one-component photoinitiating systems for the polymerization of an acrylate monomer i.e. TMPTA were studied under a LED@405 nm at room temperature. Typical acrylate conversion vs. irradiation time profiles are shown in Figure 2 for the 1-10 series and the associated final acrylate function conversions (FCs) are summarized in Table 2. Polymerization profiles of the 1'-10' series can be found in SI.

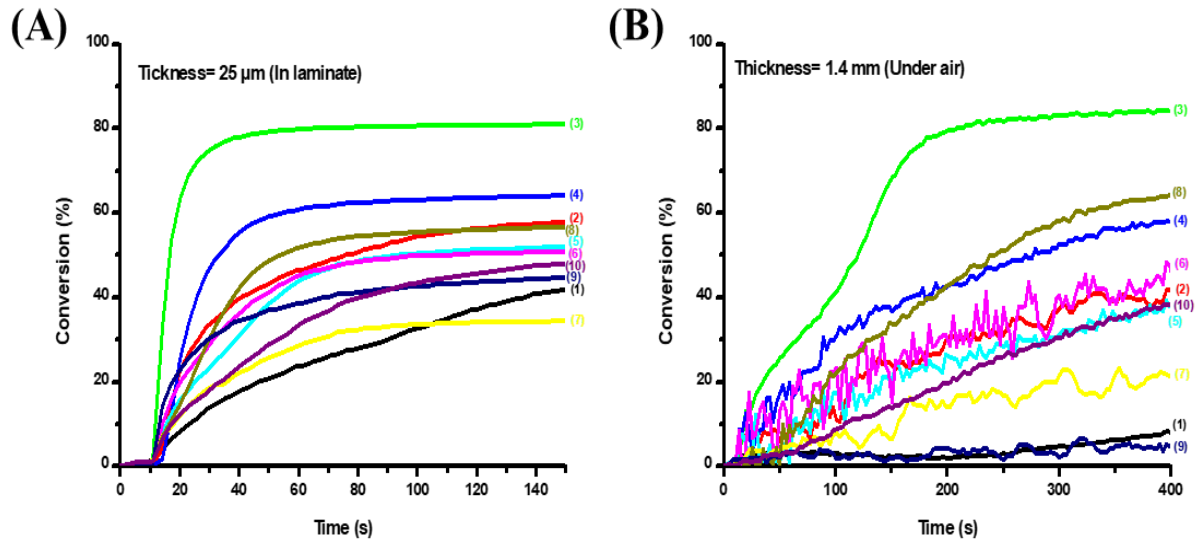

Figure 2. (A) Polymerization profiles of oxime esters **(1)-(10)** (0.5% w) in TMPTA (acrylate function conversion vs. irradiation time) in laminate (thickness = 25 µm) upon exposure to LED light λ = 405 nm ~~in the presence of one-component photoinitiating systems (0.5% w)~~. The irradiation starts after t = 10 s. (B) Polymerization profiles of oxime esters **(1)-(10)** (0.5% w) in TMPTA (acrylate function conversion vs. irradiation time) under air (thickness = 1.4 mm) upon exposure to LED light λ = 405 nm ~~in the presence of one-component photoinitiating systems (0.5% w)~~. The irradiation starts after t = 10 s.

Table 2. Final acrylate function conversions (FCs) and polymerization rates for TMPTA using one component (0.5% w) photoinitiators for compounds **(1) (10)** after irradiation with LED light (λ= 405 nm).

OXE	Thin sample (25 µm) in laminate	Thick sample (1.4 mm) under air
(1)	42%	8%
(2)	58%	50%
(3)	81%	84%
(4)	64%	58%
(5)	52%	39%
(6)	51%	45%
(7)	35%	21%
(8)	57%	65%
(9)	45%	5%
(10)	48%	39%

FRP of TMPTA in presence of the compound **(1)** (without the oxime-ester function) for thin (25 µm, in laminate) or thick (1.4 mm, under air) samples does not lead to efficient polymerization (Figure 2; table 2) compared to the other compounds. This clearly highlights the importance of the oxime-ester function to act as a Type I photoinitiator.

The oxime-ester **(3)** (with a methyl substituent on the carboxyl side) reaches the highest final conversion of 81% for thin samples and 84% for thick samples. The trend of the efficiency of the OXEs in the one-component system in thin samples (25 µm, in laminate) is **(3) > (4) > (2) > (8) > (5) > (6) > (10) > (9) > (1) > (7)**, which is not directly linked to their absorption properties. Indeed, we have also shown in our previous work (devoted to a series of coumarin-based oxime-esters) [10] the importance of other factors in the photopolymerization process, such as the cleavage reaction, the decarboxylation reaction, and the reactivity of the generated radicals. For example, the decarboxylation reaction is affected by the ester group and the reaction is energetically more favorable in the case of methyl substituent ($\Delta H_{decarboxylation}$= -4.94 kcal.mol^{-1}). [10] In addition, solubility can also affect the photoinitiation ability. For example,

compound **(9)** which possesses the highest absorption properties, is not efficient in photopolymerization, due to its poor solubility in resins. We noticed that compound **(3)** is the most soluble molecule compared to the other compounds studied, in full agreement with the study that showed that on the carboxyl side of the oxime ester, anything larger than the methyl group generally reduces the solubility. [32] The difference in reactivity (notably in terms of polymerization rate) between thin and thick samples can be attributed to an inner filter effect.

Influence of the solubility issue on the photoinitiating ability was examined by comparing the photopolymerization results of **(1)-(10)** with that of a second series **(1')-(10')** designed to exhibit a lower solubility. ~~Notably, alkylation of the carbazole moiety of this second series was carried out with methyl iodide instead of hexyl iodide. The synthesis of this second series of dyes is fully detailed in the SI.~~ As a result of this, a severe reduction of the solubility of dyes could be clearly evidenced in resins. As shown in the Table 3 and in the Figure Sxxx, important variations of the TMPTA conversions could be obtained between the two series. In thin samples, the most important variations of monomer conversions were observed between **(2)** and **(2')**, **(6)** and **(6')**, and **(9)** and **(9')** bearing oxime esters based on benzoyl, 4-methylbenzoyl or 4-nitrobenzoyl groups. Notably, a reduction as high as 17% could be detected between **(9)** and **(9')**, the nitro groups being well-known to adversely affect the solubility of dyes. In thick films, an opposite situation was found since an improvement of the monomer conversion could be detected for 6 dyes of the series. For dyes **(2')**, **(6')**, **(7')** and **(9')**, an enhancement of ca.15% monomer conversion could be demonstrated compared to their **(2)**, **(6)**, **(7)** and **(9)** analogues. These improvements can be assigned to ……

Table 3. Final acrylate function conversions (FCs) and polymerization rates for TMPTA using one component (0.5% w) photoinitiators after irradiation with LED light (λ= 405 nm).

OXE	Thin sample (25 µm) in laminate	OXE	Thin sample (25 µm) in laminate	OXE	Thick sample (1.4 mm) under air	OXE	Thick sample (1.4 mm) under air
(1)	42%	**(1')**	29%	**(1)**	8%	**(1')**	15%
(2)	58%	**(2')**	38%	**(2)**	50%	**(2')**	61%
(3)	81%	**(3')**	82%	**(3)**	84%	**(3')**	81%
(4)	64%	**(4')**	66%	**(4)**	58%	**(4')**	38%
(5)	52%	**(5')**	49%	**(5)**	39%	**(5')**	34%
(6)	51%	**(6')**	41%	**(6)**	45%	**(6')**	58%
(7)	35%	**(7')**	47%	**(7)**	21%	**(7')**	35%

(8)	57%	**(8')**	54%	**(8)**	65%	**(8')**	54%
(9)	45%	**(9')**	28%	**(9)**	5%	**(9')**	19%
(10)	48%	**(10')**	49%	**(10)**	39%	**(10')**	41%

3.4. Steady state and time resolved fluorescence to study S_1 properties

To assess the properties related to the S_1 singlet excited states of the investigated structures, steady state fluorescence analyses in toluene were performed. No fluorescence property was observed for compound **(9)**. Absorption and emission spectra of compound **(3)** and also its analysis by time-correlated single-photon counting (S_1 lifetime) are presented in Figure 3 and the data for all the other OXEs are summarized in Table 4.

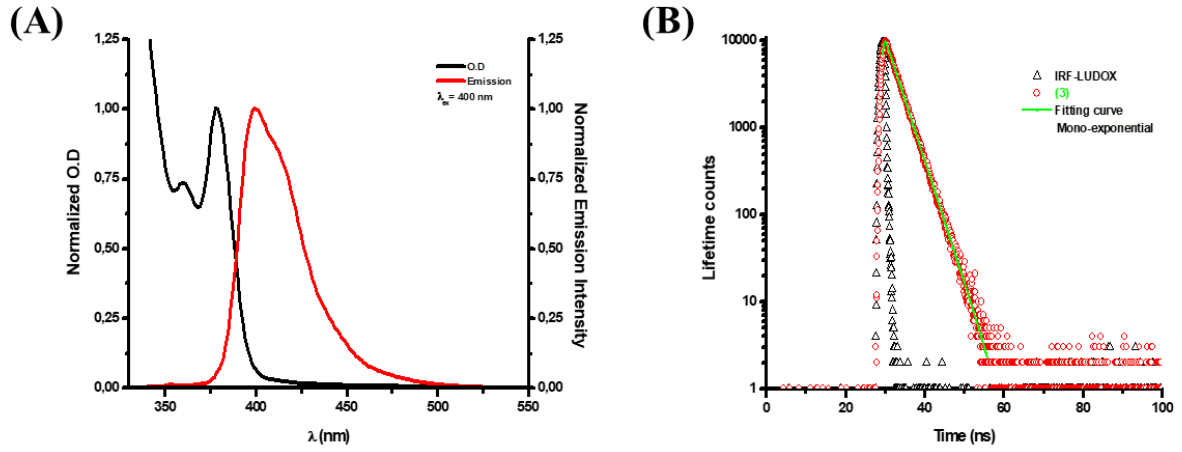

Figure 3. (A) UV-visible absorption and emission spectra of compound **(3)** in toluene. (B) Time correlated single-photon counting of **(3)** in toluene, λ_{ex}= 367 nm, λ_{em}= 400 nm, mono-exponential curve fitting.

Compound **(1)** (without the oxime-ester function) has a lifetime of 3.36 ns, which is slightly reduced after the introduction of the oxime-ester function (for the other compounds, except for compound **(10)**), suggesting cleavage from S_1, in full agreement with an energetically favorable process from S_1 ($(\Delta H_{cleavage\ S1}$= BDE (N-O) – E_{S1}) (see Table 4). In addition, the calculated triplet state energy levels for all OXEs are higher than their N-O bond dissociation energy (Table 4), which also suggests cleavage from the triplet state. Enthalpies of the cleavage process from the triplet state T_1 ($\Delta H_{cleavage\ T1}$= BDE (N-O) – E_{T1}) are all favorable (Table 4).

Table 4. Parameters characterizing the investigated OXEs **(1)-(10)**. Some parameters were calculated by molecular modelling: the bond dissociation energy BDE (N-O), the triplet state energy E_{T1} and the enthalpy $\Delta H_{cleavage\ T1}$ for the cleavage from T_1. The singlet excited state energy E_{S1}, the enthalpy $\Delta H_{cleavage\ S1}$ for the cleavage from S_1, and the fluorescence lifetime of the OXEs were measured experimentally.

OXE	BDE (N-O) (kcal.mol^{-1})	E_{S1} (kcal mol^{-1})	$\Delta H_{cleavage\ S1}$ (kcal mol^{-1})	τ_0 (S_1) (ns)	E_{T1} (kcal mol^{-1})	$\Delta H_{cleavage\ T1}$ (kcal mol^{-1})
(1)	-	74.25	-	3.25	62.21	-
(2)	41.55	73.1	-31.55	2.9	62.22	-20.67
(3)	47.02	73.56	-26.54	3.22	52.15	-5.13
(4)	40.56	72.87	-32.31	1.43	58.09	-17.53
(5)	41.35	73.33	-31.98	2.82	52.14	-10.79
(6)	41.28	73.33	-32.05	3.01	62.16	-20.88
(7)	40.88	73.33	-32.45	2.98	62.15	-21.27
(8)	41.25	73.1	-31.85	3.04	62.20	-20.95
(9)	43.71	-	-	-	62.07	-18.36
(10)	42.97	66.88	-23.91	3.85	52.45	-9.48

3.5. Steady state photolysis

Steady-state photolysis of the OXEs was performed in toluene under light irradiation, using a LED@375 nm. It is remarkable that, for the compound **(1)** (without the oxime-ester functionality) (Figure 4 (A)) no photolysis occurred compared to the compound **(4)** (and also to the other compounds) for which an efficient photolysis with a rapid formation of photoproducts after 120 s could be evidenced (Figure 4 (B)). It clearly highlights the importance of the oxime-ester functionality to allow a photoreaction possibility, in agreement with the results observed in the photopolymerization experiments.

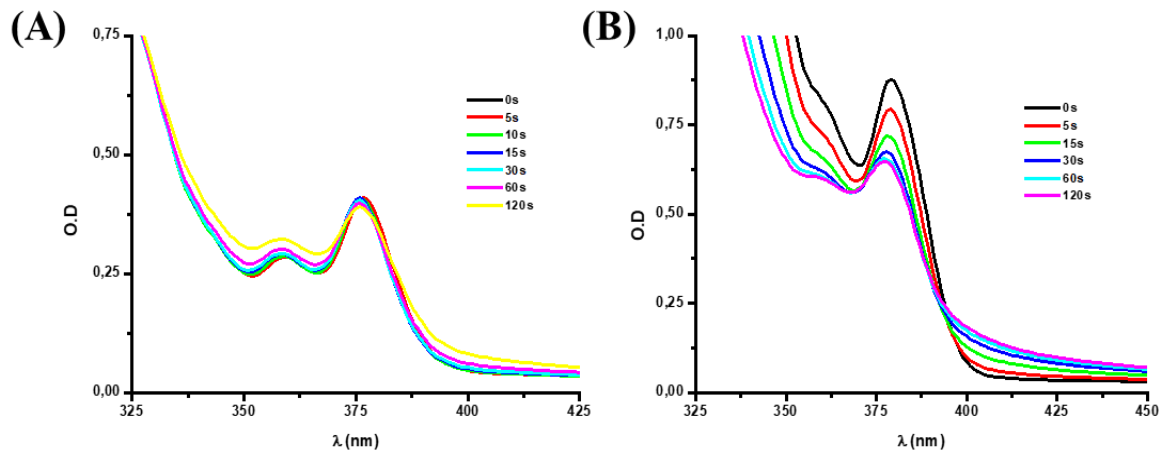

Figure 4. (A) Photolysis of compound **(1)** in toluene; (B) Photolysis of compound **(4)** in toluene.

3.6. Thermal initiator behavior

Since the studied OXEs **(1)-(10)** showed good photoinitiation abilities under LED @405nm, their thermal initiator features were also investigated, in order to highlight their dual thermal and photochemical initiator behaviors (See Figure 5). This is important especially for polymerization in shadow areas where a thermal process can overcome the problem of light penetration. The maximal, the onset polymerization temperatures, and the final acrylate function conversion of the studied structures are given in Table 5.

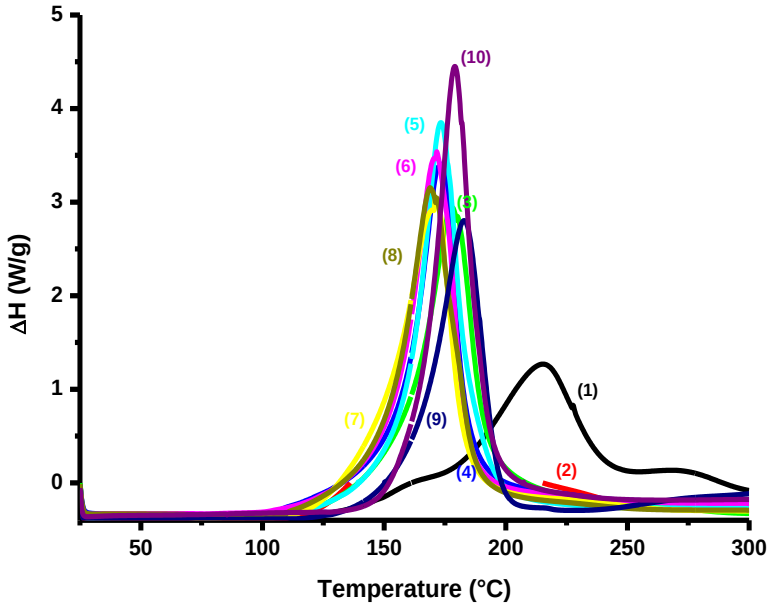

Figure 5. Thermal polymerization experiments (Enthalpy vs heating temperature) of one component initiating systems (1% w), heating rate 10 K/min, under N_2, in TMPTA.

The importance of the oxime-ester function was also demonstrated in thermal polymerization, where it can be noticed that compound **(1)** (without the oxime-ester functionality) needs a temperature of 216°C to be able to polymerize. This temperature is significantly decreased after introduction of the oxime ester function. Moreover, lower onset temperatures were also observed. This may show that the cleavage of the N-O bond is easier for the oxime-ester function.

Table 5. Maximal, onset polymerization temperatures, and final acrylate function conversion (FCs) for TMPTA using OXE (1% w) as thermal initiator under N_2.

OXE	T_{Onset} (°C)	T_{max} (°C)	Conversion (%)
(1)	112	216	62
(2)	109	175	77
(3)	108	179	71
(4)	106	176	69
(5)	110	175	74
(6)	100	174	69
(7)	110	172	75
(8)	108	171	73
(9)	114	184	59
(10)	131	181	73

3.7. 3D printing experiments

A diode laser @405 nm was used for the generation of 3D polymer patterns which were characterized by optical microscopy. This experiment was carried out under air. Especially, compounds **(3)**, **(4)**, and **(8)** (0.1% w) in TA were selected as the appropriate candidates for this experiment (see Figure 6). Remarkably, a great thickness could be obtained (~2500 μm), with a high spatial resolution (polymerization process is produced in the irradiated area) and very short irradiation times were necessary to generate the 3D patterns. In addition, 3D printing experiments were also carried out using a low light intensity 3D printer (LCD-based 405 nm 3D Printer Anycubic Photon S) showing the high photosensitivity of compound **(3)** (See Figure 6, (D)).

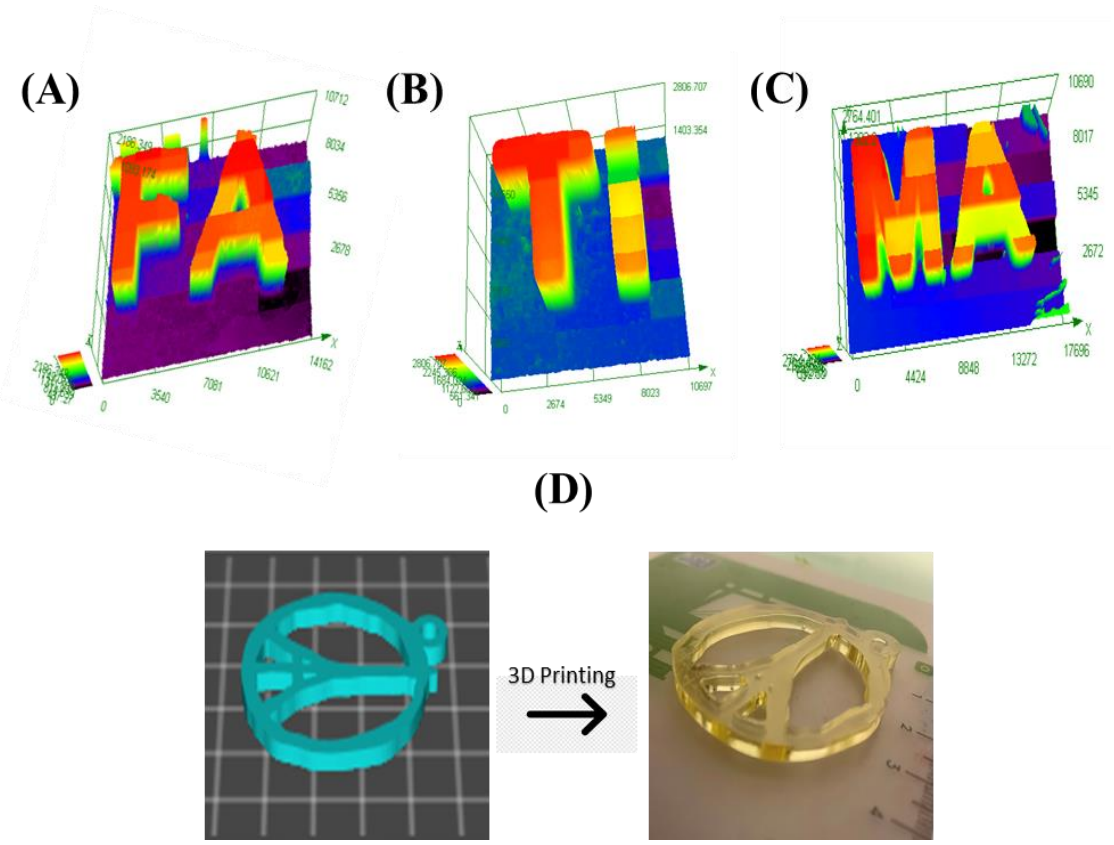

Figure 6. Free radical photopolymerization experiments @405 nm for the generation of 3D patterns characterized by numerical optical microscopy: (A) Compound **(3)** (0.1% w) in TA, (B) Compound **(4)** (0.1% w) in TA, (C) Compound **(8)** (0.1% w) in TA and (D) 3D printing experiments using a 3D printer for compound **(3)** (0.5% w) in TA.

4. Conclusion

In this article, eighteen oxime esters based on the 5,12-dihexyl-5,12-dihydroindolo[3,2-*a*]carbazole-based scaffold and varying by the ester group substitution were successfully synthetized and used as novel photoinitiators capable of initiating high-performance photopolymerization. Synthesis of the studied compounds as well as their initiation abilities as Type I photoinitiators are reported and thoroughly evaluated by means of different spectroscopic techniques. Based on their light absorption properties, cleavage ability, decarboxylation reaction as well as the reactivity of the generated radicals, some pertinent structure/efficiency relationships could be established and discussed. In addition, the thermal initiator feature was also tested, demonstrating their dual thermal/photochemical initiator behaviors. Markedly, the high performance of the newly proposed oxime-esters in initiating systems was also shown by developing highly reactive photosensitive 3D printing activable at 405 nm. Other dual thermal/photochemical initiators will be presented in forthcoming studies.

5. References

[1] E. Vessally, H. Saeidian, A. Hosseinian, L. Edjlali, A. Bekhradnia, A review on synthetic applications of oxime esters, Current Organic Chemistry, 2017, 21.3, 249-271.

[2] Y. Gao, J. Song, S. Shang, D. Wang, J. Li, Synthesis and antibacterial activity of oxime esters from dihydrocumic acid, BioResources, 2012, 7.3, 4150-4160.

[3] D. Wang, S. Ren, H. Wang, H. Yan, J. Feng, X. Zhang, Semisynthesis and antifungal activity of novel oxime ester derivatives of carabrone modified at C (4) against Botrytis cinerea, Chemistry & biodiversity, 2014, 11.6, 886-903.

[4] J. Xu, G. Ma, K. Wang, J. Gu, S. Jiang, J. Nie, Synthesis and photopolymerization kinetics of oxime ester photoinitiators, Journal of Applied Polymer Science, 2012, 123.2, 725-731.

[5] W. Qiu, J. Zhu, K. Dietliker, Z. Li, Polymerizable Oxime Esters: An Efficient Photoinitiator with Low Migration Ability for 3D Printing to Fabricate Luminescent Devices, ChemPhotoChem, 2020, 4.11, 5296-5303.

[6] C. Oh, M. Lee, W. J. Lee, Y. Cho, S. R. Shin, J. I. Shin, S. Lee, K. Jun, Novel β-oximester fluorene compound, a photopolymerization initiator comprising same, and photoresist composition. WIPO Patent WO2015108386A1, 2015.

[7] S. R. Shin, K. Jun, J. I. Shin, S. Y. Park, K. L. An, S. So. Lee, B. S. Moon, B. C. Oh, A. Choi, I. Y. So, Novel fluorene oxime ester compound, photopolymerization initiator and photoresist composition containing the same. U. S. Patent US20150111152A1, 2015.

[8] W. Wang, M. Jin, H. Pan, D. Wan, Remote Effect of Substituents on the Properties of Phenyl Thienyl Thioether-based Oxime Esters as LED-sensitive Photoinitiators, Dyes and Pigments, 2021, 109435.

[9] Z.H. Lee, F. Hammoud, A. Hijazi, B. Graff, J. Lalevée, Y.C. Chen, Synthesis and free radical photopolymerization of triphenylamine-based oxime ester photoinitiators, Polymer Chemistry, 2021, 12, 1286-1297.

[10] F. Hammoud, N. Giacoletto, G. Noirbent, B. Graff, A. Hijazi, M. Nechab, D. Gigmes, F. Dumur, J. Lalevée, Substituent Effects on Photoinitiation Ability of Coumarin-Based Oxime-

Ester Photoinitiators for Free Radical Photopolymerization, Materials Chemistry Frontiers, 2021.

[11] J. P. Fouassier, Photoinitiation, Photopolymerization, and Photocuring: Fundamentals and Applications, Hanser Publishers, New York 1995.

[12] C. Dietlin, S. Schweizer, P. Xiao, J. Zhang, F. Morlet-Savary, B. Graff, J. P Fouassier, J. Lalevée, Photopolymerization upon LEDs: new photoinitiating systems and strategies, Polymer Chemistry, 2015, 6.21, 3895-3912.

[13] P. Garra, C. Dietlin, F. Morlet-Savary, F. Dumur, D. Gigmes, J.P. Fouassier, J. Lalevée, Photopolymerization processes of thick films and in shadow areas: a review for the access to composites, Polymer Chemistry, 2017, 8.46, 7088-7101.

[14] J. P. Fouassier, J. Lalevée, Photoinitiators: Structures, Reactivity and Applications in Polymerization, Wiley, Weinhein, 2021.

[15] J. Lalevée, J. P. Fouassier, Dye Photosensitized Polymerization Reactions: Novel Perspectives, RSC Photochemistry Reports, Ed. A. Albini, E. Fasani, Photochemistry, London, UK, 2015, 215–232.

[16] Y. Yagci, S. Jockusch, N. J. Turro, Photoinitiated polymerization: advances, challenges, and opportunities, Macromolecules, 2010, 43, 6245-6260.

[17] A. AL Mousawi, F. Dumur, P. Garra, J. Toufaily, T. Hamieh, F. Goubard, T.T. Bui, B. Graff, D. Gigmes, J.P. Fouassier, J. Lalevée, Azahelicenes as Visible Light Photoinitiators for Cationic and Radical Polymerization: Preparation of Photoluminescent Polymers and Use in High Performance LED Projector 3D Printing Resins, Journal of Polymer Science, 2017, Part A, 55, 1189–1199.

[18] F. Karasu, C. Croutxé-Barghon, X. Allonas, D. V. Van, G. J. Leendert, Free radical photopolymerization initiated by UV and LED: Towards UV stabilized, tack free coating, J Polym Sci, Part A: Polym Chem, 2015, 52.24, 3597-607.

[19] N. Zivic, M. Bouzrati, S. Villote, F. Morlet-Savary, C. Dietlin, F. Dumur, D. Gigmes, J.P. Fouassier, J. Lalevée, A novel naphthalimide scaffold based iodonium salt as a one-component photoacid/photoinitiator for cationic and radical polymerization under LED exposure, Polymer Chemistry, 2016, 7, 5873-5879.

[20] D. E. Fast, A. Lauer, J. P. Menzel, A. M. Kelterer, G. Gescheidt, C. Barner-Kowollik, Wavelength-Dependent Photochemistry of Oxime Ester Photoinitiators, Macromolecules, 2017, 50, 1815-1823.

[21] S. Chen, M. Jin, J.P. Malval, J. Fu, F. Morlet-Savary, H. Pan, D. Wan, Substituted stilbene-based oxime esters used as highly reactive wavelength-dependent photoinitiators for LED photopolymerization, Polymer Chemistry, 2019, 10.48, 6609-6621.

[22] W. Qiu, M. Li, Y. Yang, Z. Li, K. Dietliker, Cleavable coumarin-based oxime esters with terminal heterocyclic moieties: photobleachable initiators for deep photocuring under visible LED light irradiation, Polymer Chemistry, 2020, 11.7, 1356-1363.

[23] K. Sun, C. Pigot, H. Chen, M. Nechab, D. Gigmes, F. Morlet-Savary, B. Graff, S. Liu, P. Xiao, F. Dumur, J. Lalevée, Free Radical Photopolymerization and 3D Printing Using Newly Developed Dyes: Indane-1,3-Dione and 1H-Cyclopentanaphthalene-1,3-Dione Derivatives as Photoinitiators in Three-Component Systems, Catalysts, 2020, 10, 463.

[24] F. Hammoud, Z.H. Lee, B. Graff, A. Hijazi, J. Lalevée, Y.C. Chen, Novel phenylamine-based oxime ester photoinitiators for LED-induced free radical, cationic, and hybrid polymerization, Journal of Polymer Science, 2021, 59, 1711–1723.

[25] M Abdallah, D Magaldi, A Hijazi, B Graff, F Dumur, JP Fouassier, TT Bui, F Goubard, J Lalevée, Development of New High-Performance Visible Light Photoinitiators Based on Carbazole Scaffold and Their Applications in 3D Printing and Photocomposite Synthesis, J. Polym. Sci., Part A, 2019, 57, 2081–2092.

[26] Z. Li, X. Zou, G. Zhu, X. Liu, R. Liu, Coumarin-based oxime esters: photobleachable and versatile unimolecular initiators for acrylate and thiol-based click photopolymerization under visible light-emitting diode light irradiation, ACS applied materials & interfaces, 2018, 10.18, 16113-16123.

[27] X. Y. Ma, R. Q. Gu, L. J. Yu, W. X. Han, J. Li, X. Y. Li, T. Wang, Conjugated phenothiazine oxime esters as free radical photoinitiators, Polymer Chemistry, 2017, 8, 6134-6142.

[28] Z. H. Lee, T. L. Huang, F. Hammoud, C.C. Chen, A. Hijazi, B. Graff, J. Lalevée, Y. Chen, Effect of the Steric Hindrance and Branched Substituents on Visible Phenylamine Oxime Ester Photoinitiators: Photopolymerization Kinetics Investigation through Photo-DSC Experiments. Photochemistry and Photobiology. 2021.

[29] S. Liu, B. Graff, P. Xiao, F. Dumur, J. Lalevée, Nitro-Carbazole Based Oxime Esters as Dual Photo/Thermal Initiators for 3D Printing and Composite Preparation, Macromolecular Rapid Communications, 2021, 2100207.

[30] P. Hu, W. Qiu, S. Naumov, T. Scherzer, Z. Hu, Q. Chen, W. Knolle, Z. Li, Conjugated bifunctional carbazole-based oxime esters: Efficient and versatile photoinitiators for 3D Printing under one-and two-photon excitation. ChemPhotoChem, 2020, 4.3, 224-232.

[31] R. Zhou, H. Pan, D. Wan, J. P. Malval, M. Jin, Bicarbazole-based oxime esters as novel efficient photoinitiators for photopolymerization under UV-Vis LEDs. Progress in Organic Coatings, 2021, 157, 106306.

[32] W. J. Lee, H. S. Kwak, D. Lee, C. Oh, E. K. Yum, Y. An, M. D. Halls, C. W. Lee, Design and synthesis of novel oxime ester photoinitiators augmented by automated machine learning, Chemistry of materials, 2021.